

Shear behavior of fibrous concrete beams reinforced by GFRP

Ali Alsajaad Ibrahim¹
ali199963110@gmail.com

Hassan Falah Hassan²
hassanfalah@uomustansiriyah.edu.iq

Mohammad Hussein Kadem³
mohammed.aldahlalei@gmail.com

Abstract: The “Glass Fiber reinforced Polymers (GFRP)” can be used to produce reinforcement bars that can be used as good alternatives for conventional steel reinforcement due to its reasonable strength / weight ratio and corrosion resistance. The “Fiber Reinforced Concrete (FRC)” is such kind of concrete that can be fabricated by the addition of steel fibers into concrete mix in order to enhance the mechanical potential and the consequent structural performance. This study was presented to inspect the shear performance of fibrous concrete beams that reinforced by GFRP bars and stirrups. The experimental program cast and test sixteen reinforced concrete beams. Fifteen beams were reinforced by GFRP stirrups and one beam was reinforced by steel stirrups as a reference beam. The variables of this study comprised the amount of steel fibers, shear reinforcement ratio and concrete compressive strength, the beam was divided to five groups according to test parameters. Experimental results showed that Increasing shear reinforcement ratio from 0.444% to 0.887% increases the failure load by 8, 9 and 11% for steel fiber content 0, 0.5 and 1% , respectively. Also results showed that increasing concrete compressive strength from 30 MPa to 70 MPa increases the failure load by 27, 40 and 42% for steel fiber content 0, 0.5 and 1% , respectively. Increasing steel fibers content from 0 to 1% increases the failure load by 8 to 18.9%. The increases in concrete compressive strength from 30 to 70 MPa decrease the strain in GFRP stirrups between (60-125%), while the increase in shear reinforcement ratio from 0.444 to 0.887 decreases the strain in stirrups GFRP bars between (5-64%). The increase in steel fibers content leads to decrease

¹ M.Sc. Student: Civil Engineering Department, Faculty of Engineering, Mustansiriyah University, Baghdad, Iraq

² Prof. Dr.: Civil Engineering Department, Faculty of Engineering, Mustansiriyah University, Baghdad, Iraq

³ Assist. Prof. Dr.: Civil Engineering Department, Faculty of Engineering, Mustansiriyah University, Baghdad, Iraq

in concrete compressive strain between (71.5-301 %). The increases in concrete compressive strength from 30 to 70 MPa decrease in concrete compressive strain between (25.8-269%). Crack width were decreased by (32-108%) when the steel fibers content increased from 0 to 1% for all tested beams. Experimental results showed that increase steel fibers content and shear reinforcement ratio decrease the ultimate concrete compressive strain. Results showed that the ductility index by deformability approach decreases with the increase of the steel fibers content due to increase the moment and deflection at ($\epsilon_{cu}=0.001$). The comparison of experimental and calculated ultimate shear load showed that the CSA and ISIS codes result were very conservative with safety factor reaching to 66%, the experimental results showed good agreement to the ACI and Tureyen while equation code results.

Keywords: FRC, GFRP, Concrete Beams, Reinforcement

1. Introduction

Deterioration of concrete structures due to the corrosion of steel reinforcement has lead to the need for an alternative type of reinforcement such as fiber-reinforced-polymer (FRP) reinforcement. Stirrups used for shear reinforcement are normally located as an outer reinforcement with respect to the flexural reinforcement and therefore are more susceptible to severe environmental effects because of the minimum concrete cover provided. FRPs are corrosion-free materials and have recently been used as reinforcement to avoid the deterioration of concrete structures caused by corrosion of steel reinforcement. Use of FRP as reinforcement for concrete structures has increased rapidly over the last ten years. FRP reinforcement is made from high-tensile-strength fibers such as carbon, glass, aramid and others embedded in polymeric matrices and produced in the form of bars, strands ropes, tendons and grids, in a wide variety of shapes and characteristics. FRP reinforcement is used as prestressed, non-prestressed and shear reinforcement for concrete structures. Several experimental and analytical research programs have been conducted to investigate the flexural behavior of concrete members reinforced and/or prestressed by FRP reinforcement. The use of FRP as shear reinforcement for concrete structures has not yet been fully explored and the currently available data are not sufficient to formulate rational design guidelines [1-5].

Since FRP reinforcement is characterized by a linearly elastic stress-strain relationship up to failure, shear failure of reinforced concrete members will occur due either to rupture of FRP stirrups or to crushing of concrete in the compression zone or in the web. Failure due to rupture of FRP stirrups will occur suddenly

when one or more FRP stirrups reach their strength capacity. This type of shear failure is brittle when compared to that of a beam reinforced with steel stirrups. The other mode of failure, shear-compression failure, occurs when the diagonal shear cracks propagate towards the compression chord, reducing the depth of the compression zone and causing crushing of the concrete. Such a mode of failure is much more comparable to that of a concrete beam with steel stirrups. Concrete members reinforced with steel stirrups are normally designed for shear to allow yielding of the steel stirrups before crushing of concrete. Due to the diagonal nature of shear cracks, the induced tensile forces are typically oriented at an angle with respect to the stirrups and consequently the stirrups' tensile strength in the direction of the fibers may not be developed. Bending of FRP stirrups to develop sufficient anchorage may also lead to a significant reduction in the strength capacity of the stirrups [6-10].

2. Test Specimens

Sixteen beams were cast and test in this research. Each simply support concrete beam with a rectangular section of 150×200 mm with a total length of 1550 mm. The beams were simply support over one span of 1450 mm center to center between two supports and a 50 mm overhang. All the beams were reinforced by 3- ϕ 16 of GFRP bars as bottom tension reinforcement. Figure 1 shows details of tested beam. The studied parameters in the test were:

- Shear reinforcement ratio (ρ_{vf}).
- Concrete compressive strength.
- Steel fiber content (V_f).

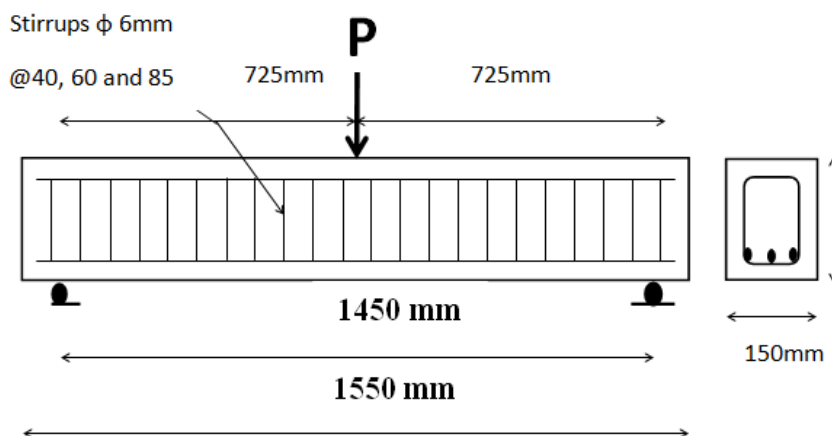


Figure 1: Details of tested beam

Beams designations were as follows:

(B) For the beam

(R) Reference

(30, 50 and 70) for the compressive strength of concrete.

(0.5d, 0.33d, and 0.25d) for change spacing in stirrups.

(0%, 0.5% and 1%) for steel fiber content.

For example, the following code (B30-0.5d-0) indicates that the beam has a concrete compressive strength of 30 MPa. The spacing of stirrup (0.5d), 0% steel fiber content. Table 1 shows details of the tested beams.

Table 1: Properties of the tested beams

Beam specimen	Target concrete strength (MPa)	Steel Fiber %	Stirrups spacing (mm)
BR30-0.5d-0	30	0.0	6@85 ^a
B30-0.5d-0		0.0	
B30-0.5d-0.5	30	0.5	6@85
B30-0.5d-1		1.0	
B30-0.33d-0	30	0.0	6@60
B30-0.33d-0.5		0.5	
B30-0.33d-1		1.0	
B30-0.25d-0		0.0	
B30-0.25d-0.5	30	0.5	6@40
B30-0.25d-1		1.0	
B50-0.5d-0		0.0	
B50-0.5d-0.5	50	0.5	6@85
B50-0.5d-1		1.0	
B70-0.5d-0	70	0.0	6@85
B70-0.5d-0.5		0.5	
B70-0.5d-1		1.0	

^a Reference beam with steel stirrups.

3. FRPs as a Structural Element

As a structural reinforcement, FRPs was recognized to be utilized in different shapes and forms in structures such as:

1. FRP sheets: were thin, flexible and light in weight. sheets were mainly used for strengthening and retrofitting of an existing structural element by increasing its bearing capacity without the need for drilling concrete to add

additional reinforcement. This provides a very beneficial solution for the structural element that requires a change in function. FRP sheet along with its application can be shown in Figure 2.



Figure 2: FRP Sheets

2. FRP Bars: Many kinds of rebars with different treated surfaces are available nowadays with a lighter weight and much greater tensile strength than the conventional steel reinforcement. Different FRP rebars are shown in Figure 3.



Figure 3: A different type of FRP rebar

3. FRP Macro-fibers: The FRP can also be fabricated as a randomly oriented and discrete fibers known as chopped fiber added to the concrete in order to provide the concrete with higher durability and more ability to resist the

damaging effects of loads, especially under tensile loadings. These fibers can be depicted from Figure 4.



Figure 4: FRP Macro-fibers

4. Mix Proportions

Concrete mixtures were obtained by preparing locally available raw materials such as cement, sand, gravel, water ... etc.. Mixing the materials with using the electric mixer available in the laboratory was with a 0.20m³ capacity as can be seen from [11]. The concrete production of targeted compressive strengths was of 30, 50 and 70MPa. The mixing ratios of raw materials for each mix are illustrated in Table 2. Mixtures are designed according to the ACI-211.1-91.

Control specimens were subjected from that very same mixture of concrete used to cast the beams. At the 28 days of curing, the experimental specimens are tested. The mechanical properties of experiments are shown in the Table 3.

Table 2: Mixture design characteristics

Target Concrete strength (MPa)	Cement kg/m ³	Sand kg/m ³	Gravel kg/m ³	Silica fume kg/m ³	W/C	Viscocrete PC20 kg/m ³
30	400	550	1200	---	0.45	---
50	575	880	767	45	0.3	22.5
70	650	900	500	90	0.22	26

Table 3: Mechanical Properties of concrete

No.mix	Vf %	f _c (MPa)	f _{cu} (MPa)	f _t (MPa)	f _r (MPa)	E _c (GPa)
30	0.0	31.5	33.5	3.2	3.75	24.5
	0.5	36.5	39	3.9	4.43	29.5
	1.0	40.5	43	4.2	5.25	31
50	0.0	50.75	59.55	3.5	4.9	33.5
	0.5	58.67	66.67	4.7	5.5	36
	1.0	65.45	68.33	5.4	6.12	39.5
70	0.0	71.5	78.64	4.5	5.12	40.5
	0.5	77.5	80.45	5.9	6.75	42.75
	1.0	82.98	87.55	6.7	7.25	43.5

5. Comparison between GFRP and steel reinforcement

Table (4) shows the different of experimental results of (BR30-0.5d-0 and B30-0.5 d-0), which was reinforced by the same number of stirrups and diameter and same concrete compressive strength, but different type of reinforcements, was used. Results show that the failure loads for (BR30-0.5d-0) was very close (B30-0.5d-0).

Table 4: Comparison of experimental results of GFRP and steel

BS*	RR	RT	FL	UD	US	UCW
BR30-0.5d-0	0.222	Steel	76.5	11.98	0.001424	1.33
B30-0.5d-0	0.222	GFRP	76.0	12.50	0.001930	1.56

*BS: Beam Specimen

RR: Reinforcement Ratio (%)

RT: Reinforcement Type

FL: Failure Load (P_u) (kN)

UD: Ultimate Deflection (mm)

US: Ultimate Strain

UCW: Ultimate Crack Width (mm)

6. Deflection

Figures 5 to 9 show the load-deflection relationships for all tested beams. It is observed that the increasing in steel fibers content reduce deflection at the same load level, at (76.5 KN) the deflection decreased by (2 and 33) for (B30-0.5d-0.5 and B30-0.5d-1), respectively as compared with (B30-0.5d-0).

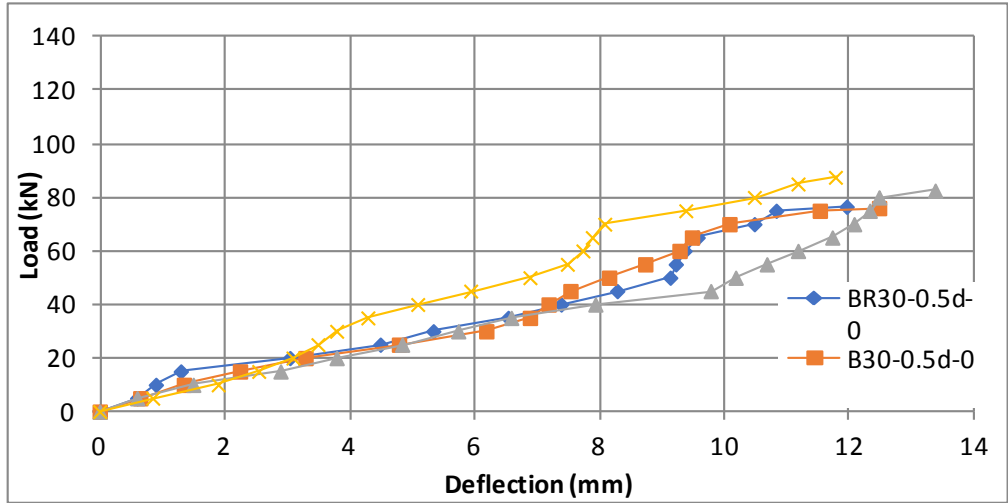


Figure 5: load experimental deflection B30-0.5d

Also at (81 kN) deflection were decreased by (15 and 17) for (B30-0.33d-0.5 and B30-0.33d-1), respectively as compared with (B30-0.33d-0).

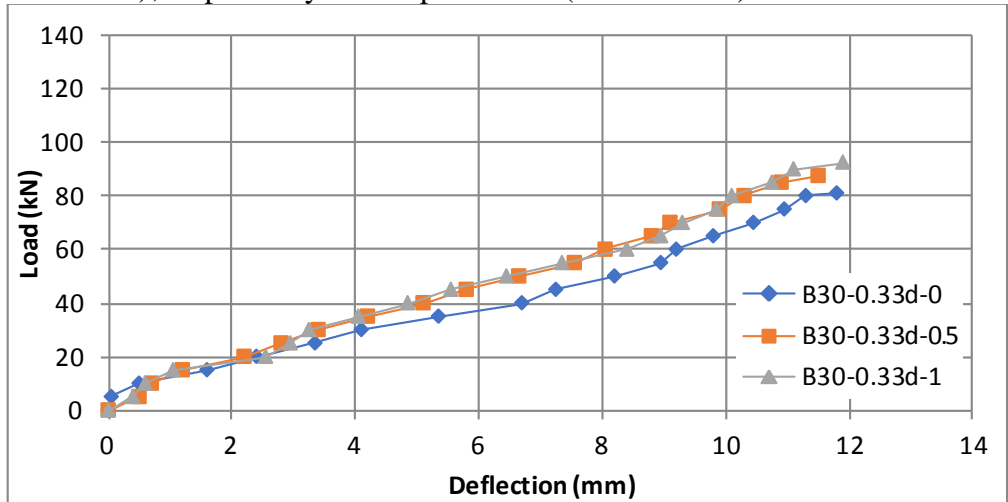


Figure 6: Load experimental deflection B30-0.33d

While at (82kN) increasing steel fiber contents form (0%) to (0.5 & 1%) loads to decrease the deflection by (3 and 31) for (B30-0.25d-0.5 and B30-0.25d-1), respectively as compared with (B30-0.25d-0).

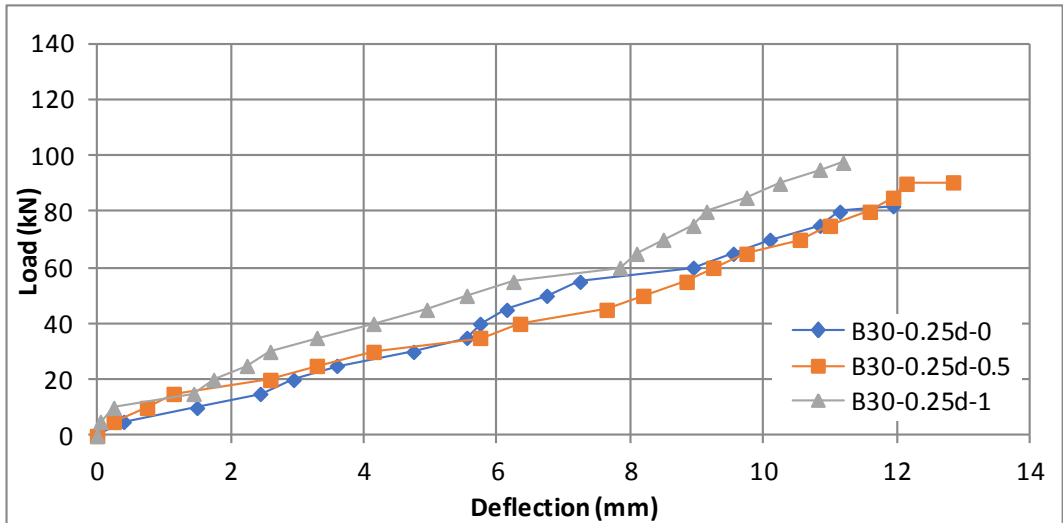


Figure 7: load experimental deflection B30-0.25d

Also at (88kN) the deflection were decreased by (33 and 49) for (B50-0.5d-0.5 and B50-0.5d-1), respectively as compared with (B50-0.5d-0) due to increasing the steel fibers content from (0%) to (1%).

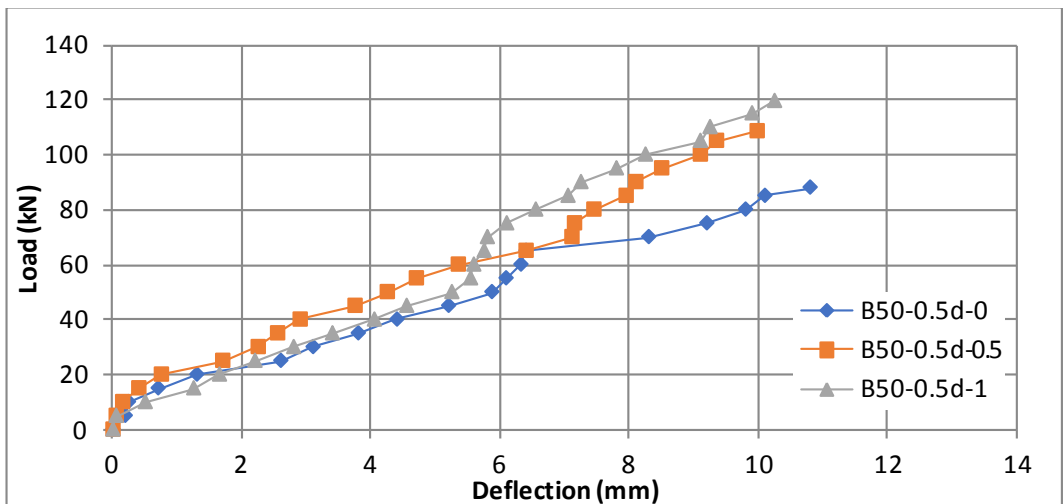


Figure 6: Load experimental deflection B50-0.5d

On the other hand at (97kN) the reduction in deflection were (11 and 20) for (B70-0.5d-0.5 and B70-0.5d-1), respectively as compared with (B70-0.5d-0).

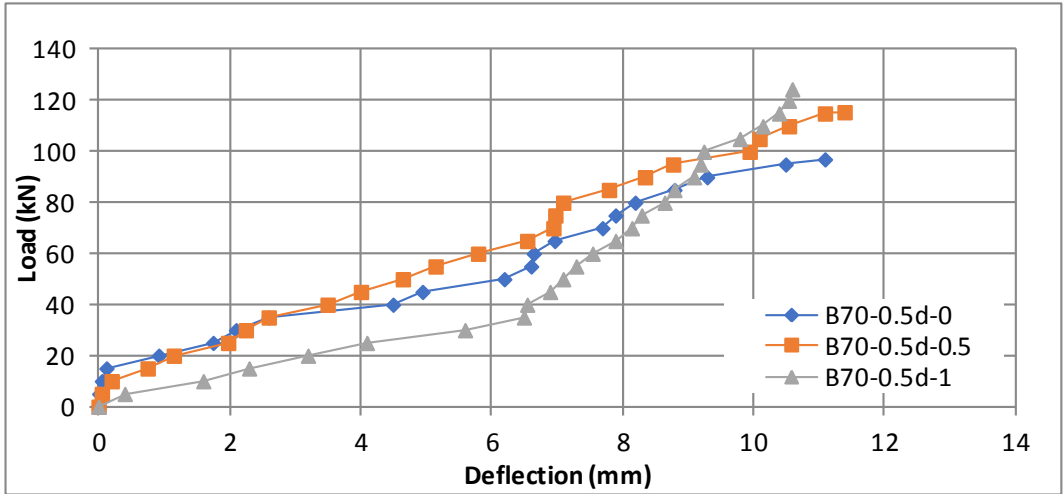


Figure 9: Load experimental deflection B70-0.5d

7. Crack width

The cracks width were measured using analyzed image by the software of creative cloud (CC) of Photoshop where an actual scale object reference has been placed at an identical distance of tested beam and after that, the image that has been captured will be analysed for the predictions of the crack width with a high degree of accuracy.

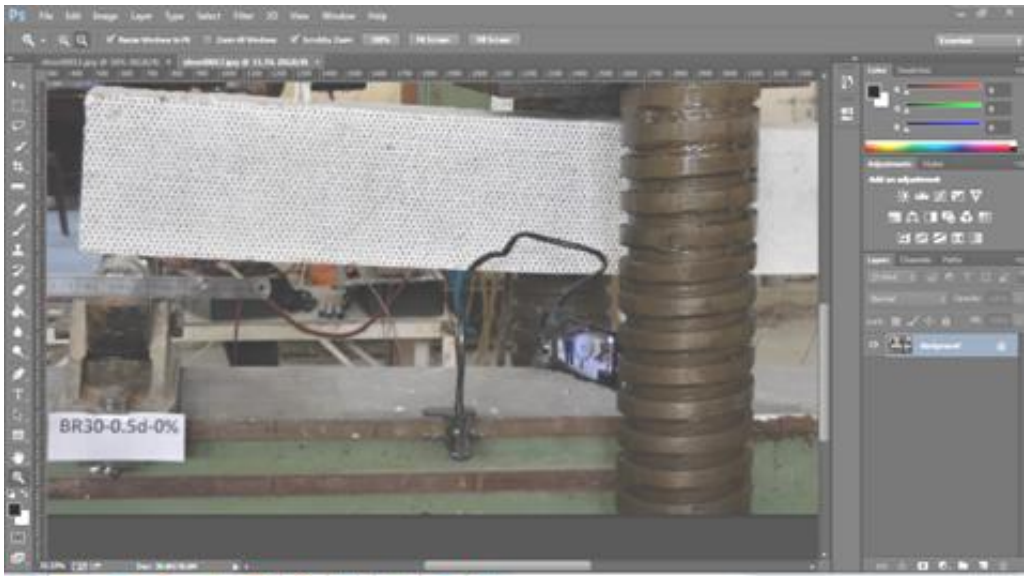


Figure 10: Crack width measurements

Figures 11 to 15 show the load-crack with relationship. The recorded results of the tests were divided to five groups based on the amount of the concrete strength and shear reinforcement of the tested beam.

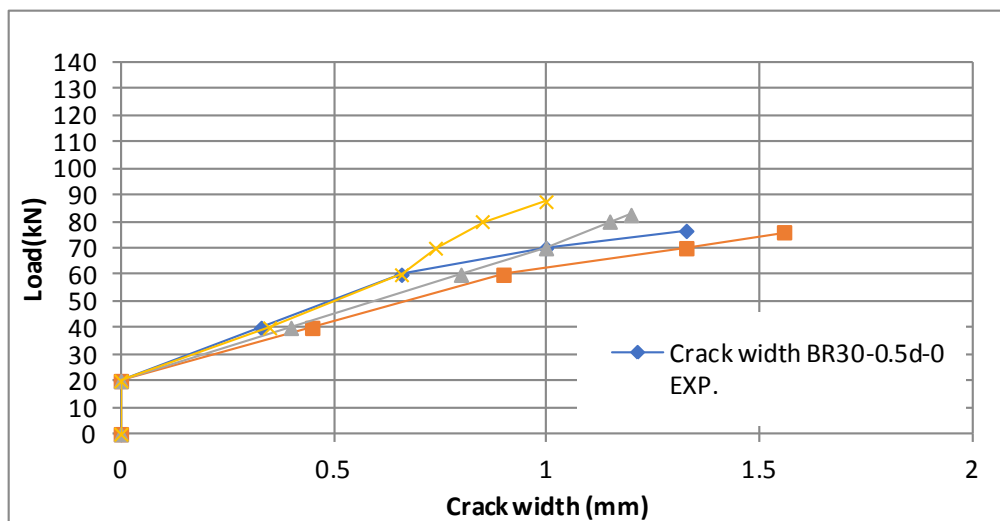


Figure 11: Load-midspan experimental crack width of B30-0.5d

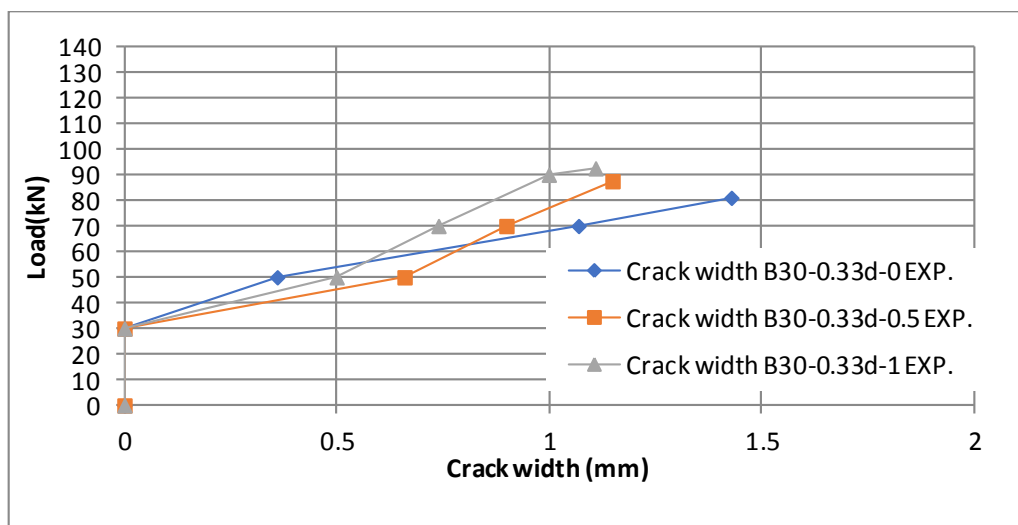


Figure 12: Load-midspan experimental crack width of B30-0.33d

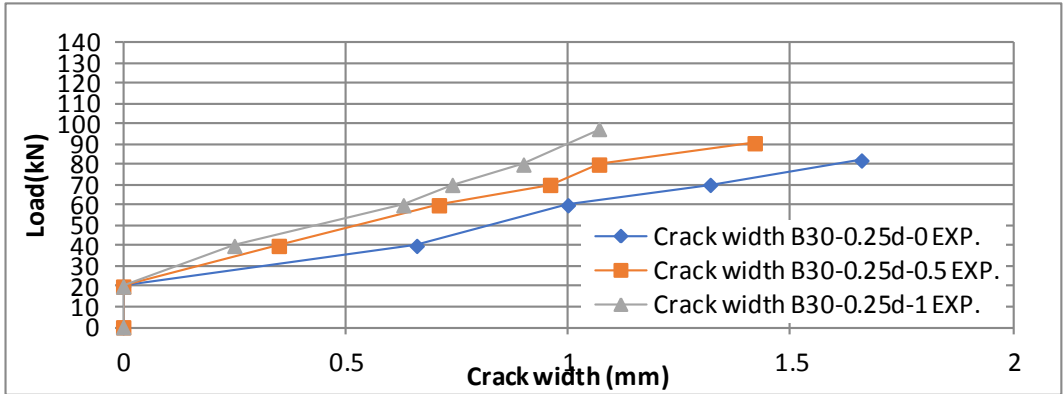


Figure 13: Load-midspan experimental crack width of B30-0.25d

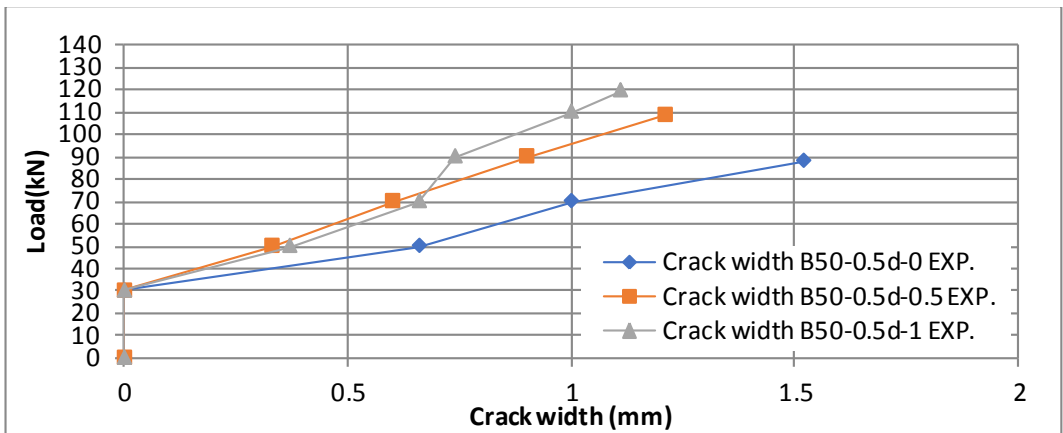


Figure 14: Load-midspan experimental crack width of B50-0.5d

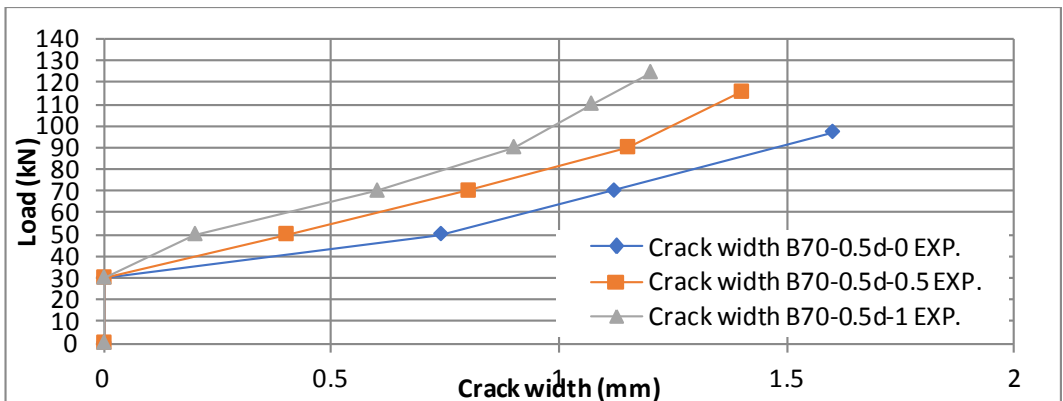


Figure 15: Load-midspan experimental crack width of B70-0.5d

At the stage of the first crack, crack load was the same value at each beam with the same steel fibers content because the width of crack at this stage depends only on concrete tensile strength. After the first crack load the width of crack would be different for each beam. This behavior is due to the increase in the amount of stress in the longitudinal reinforcement bars and accordingly, to the increase strain in these bars. At (76KN) crack width was decreased by (43 and 94%) for (B30-0.5d-0.5 and B30-0.5d-1), respectively as compared with (B30-0.5d-0) due to increasing in steel fibers content, at (81KN) crack width was decreased by (35 and 62%) for (B30-0.33d-0.5 and B30-0.33d-1), respectively as compared with (B30-0.33d-0) due to increasing in steel fibers content, at (82KN) crack width was decreased by (47 and 80%) for (B30-0.25d-0.5 and B30-0.25d-1), respectively as compared with (B30-0.25d-0) due to increasing in steel fibers content, at (88KN) crack width was decreased by (74 and 108%) for (B50-0.5d-0.5 and B50-0.5d-1), respectively as compared with (B50-0.5d-0) due to increasing in steel fibers content, at (97KN) crack width was decreased by (32 and 67%) for (B70-0.5d-0.5 and B70-0.5d-1), respectively as compared with (B70-0.5d-0).

A comparison between experimental results of cracks width with those values of the cracks width obtained based on (ACI440 -1 R -06) [12] for the beams that have been reinforced with (GFRP). The calculated crack width was accorded to the equations of the mentioned codes as follows:

$$w_{cr} = 2 \frac{f_f}{E_f} \beta k_b \sqrt{d_c^2 + \left(\frac{s}{2}\right)^2} \quad \text{ACI440 - 1R - 06} \quad \text{eq(1)}$$

Where w_{cr} represents crack width at the beam's tensile face E_f represents the elasticity modulus for reinforcement of FRP, f_f represents stress in longitudinal reinforcement of FRP, β represents coefficient to contrary size of the crack that corresponds to the reinforcement level to the beam's tensile face, k_b represents coefficient responsible for the bond degree between FRP bar and surrounding concrete, ACI440.1 R-06 [66] suggested 1.40 for the deformed fiber reinforced bars in the case where k_b isn't known experimentally, d_c represents concrete cover thickness that is measured from extreme tension fibers to a centre of closest longitudinal bars' level, and S represents bar spacing, the evaluation accuracy highly relies upon the k_b value, and approximation is on conservative side in the case where the value of $k_b = 1.40$.

The model of CEB-FIP [13] predicts the size of the crack as follows:

$$W = \beta S_m \varepsilon_m \quad \text{eq(2)}$$

$\beta = 1.30$, S_m represents average FRP reinforced member's crack spacing, m represents average reinforcement strain that permits for tension stiffening as:

$$\varepsilon_m = \sigma_s \left[1 - \frac{\beta_1 \beta_2 \left(\frac{\sigma_{sf}}{\sigma_s}\right)^2}{E_f} d \right] \quad \text{eq(3)}$$

Where σ_s represents stress in the reinforcement of the tension that has been estimated based on a cracked section. σ_{sr} represents stress in reinforcement of the tension that has been estimated according to a cracked section under load circumstances, causing 1st one of the cracks, $\beta_1 = 1.0$ for high-bond bars and 0.50 for plain ones; $\beta_2 = 1$ for the single short-term loading as well as 0.50 for the cyclic or sustained load.

ISIS Canada- 07[14] suggests the following equation for the calculation of the crack width:

$$W = 2.2k_b \frac{f_f}{E_f} \frac{h_2}{h_1} \sqrt[3]{d_c A} \quad \text{eq(4)}$$

Where K_b is bond dependent coefficient. For the fiber reinforced bars that have bond characteristics that are similar to concrete, $k_b=1$, h_2 is a distance between the extreme tension surface and NA., h_1 is the distance between tension reinforcement centroid and NA and A represents concrete's effective tension area that surrounds the reinforcement of the flexural tension and have the same centroid as this reinforcement, divided by number of the bars. Table (5) lists the calculated as well as the experimental width of the crack for all of the tested beams.

Table 5: Experimental and calculated ultimate crack width

Beam specimen	W_{exp} (mm)	W_{ACI} (mm)	$W_{CEB-FIP}$ (mm)	W_{ISIS} (mm)	$\frac{W_{exp}}{W_{ACI}}$	$\frac{W_{exp}}{W_{CEB-FIP}}$	$\frac{W_{exp}}{W_{ISIS}}$
B30-0.5d-0	1.56	0.75	0.34	0.98	2.08	4.6	1.6
B30-0.5d-0.5	1.23	0.73	0.52	0.95	1.68	2.37	1.3
B30-0.5d-1	1	0.54	1.58	0.71	1.9	0.63	1.41
B30-0.33d-0	1.45	1.46	1.15	1.89	0.99	1.26	0.77
B30-0.33d-0.5	1.15	1.45	1.36	1.88	0.79	0.85	0.61
B30-0.33d-1	1.09	1.39	1.53	1.81	0.78	0.71	0.6
B30-0.25d-0	1.66	1.17	0.92	1.52	1.42	1.80	1.09
B30-0.25d-0.5	1.42	1.11	1.049	1.45	1.28	1.35	0.98
B30-0.25d-1	1.07	1.20	1.59	1.56	0.89	0.67	0.69
B50-0.5d-0	1.52	1.12	1.21	1.45	1.36	1.26	1.05
B50-0.5d-0.5	1.21	1.37	1.62	1.78	0.88	0.75	0.68
B50-0.5d-1	1.15	1.04	1.71	1.35	1.11	0.67	0.85
B70-0.5d-0	1.6	0.96	0.13	1.06	1.67	12.31	1.51
B70-0.5d-0.5	1.2	1.21	1.43	1.57	0.99	0.84	0.76
B70-0.5d-1	1.11	0.92	1.53	1.20	1.21	0.73	0.93
Average					1.27	2.05	0.99

The calculated result showed that the CEB-FIP [13] have a good agreement with experimental result because the CEB-FIP [13] equation take in consideration the strain in longitudinal bars which effected by the parameters of study.

Generally, all available codes equation needs some modifications to be applicable for high strength and fibrous concrete.

8. Crack Patterns

The relationship between crack paths and the load applied is seen in the Figures 16 to 31. For beams (BR30-0.5d-0 ,B30-0.5d-0 , B30-0.5d-0.5,B30-0.5d-1), the first crack was a vertical curvature appeared at the midspan of beam at (21.5 , 20,22,23.5 KN),respectively. This crack continues increasing with an increase of applied load till it reaches compression area. With an increased load, new cracks are created on the two sides of the first crack and proceed to the compression area as a result of increased bending moment and shear stress. For beams (B30-0.33d-0, B30-0.33d-0.5, B30-0.33d-1), the first crack was a vertical curvature appeared at the midspan of beam at (18.5, 20, 22.5 KN), respectively. This crack keeps increasing with the increase in applied load till it reaches the compression area. With an increase of load, new cracks are appeared on the two sides of first crack and proceed to the compression area as a result of increased bending moment and shear stress. For beams (B30-0.25d-0, B30-0.25d-0.5, B30-0.25d-1), the first crack was a vertical curvature appeared at the midspan of beam at (17.5, 21.5,24 KN), respectively. This crack keeps increasing with the increased applied load to the point where it reaches the compression area. With increased load, new cracks appeared on the two sides of the first crack and proceed to the compression area as a result of increased bending moment and shear stress. For beams (B50-0.5d-0, B50-0.5d-0.5, B50-0.5d-1), the first crack was a vertical curvature appeared at the midspan of beam at (24, 25, 27KN), respectively. This crack keeps increasing with increasing the value of the applied load to the point where it reaches the compression area. With an increased load, new cracks are appeared on the two sides of the first crack and proceed to the compression area as a result of increased bending moment and shear stress. For beams (B70-0.5d-0, B70-0.5d-0.5, B70-0.5d-1), the first crack was a vertical curvature appeared at the midspan of beam at (24, 26, 27.5KN), respectively. This crack keeps increasing with an increased applied load to the point where it reaches the compression area. With an increased load value, new cracks are appeared on the two sides of first crack and proceed to the compression area as a result of increased bending moment and shear stress.

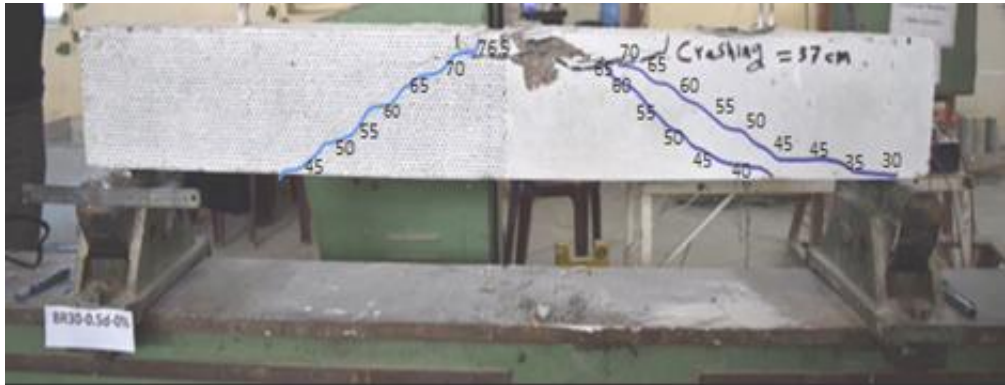


Figure 16: Crack pattern of beam (BR30-0.5d-0)



Figure 17: Crack pattern of beam (B30-0.5d-0)



Figure 18: Crack pattern of beam (B30-0.5d-0.5)



Figure 19: Crack pattern of beam (B30-0.5d-1)



Figure 20: Crack pattern of beam (B30-0.33d-0)



Figure 21: Crack pattern of beam (B30-0.33d-0.5)

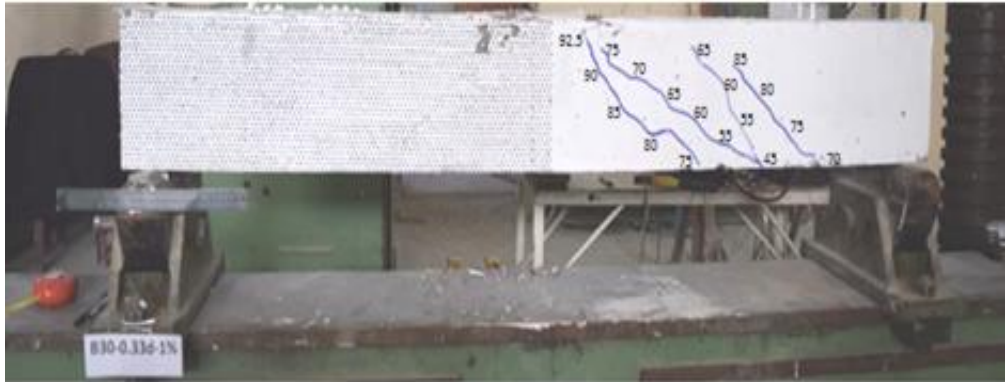


Figure 22: Crack pattern of beam (B30-0.33d-1)



Figure 23: Crack pattern of beam (B30-0.25d-0)



Figure 24: Crack pattern of beam (B30-0.25d-0.5)

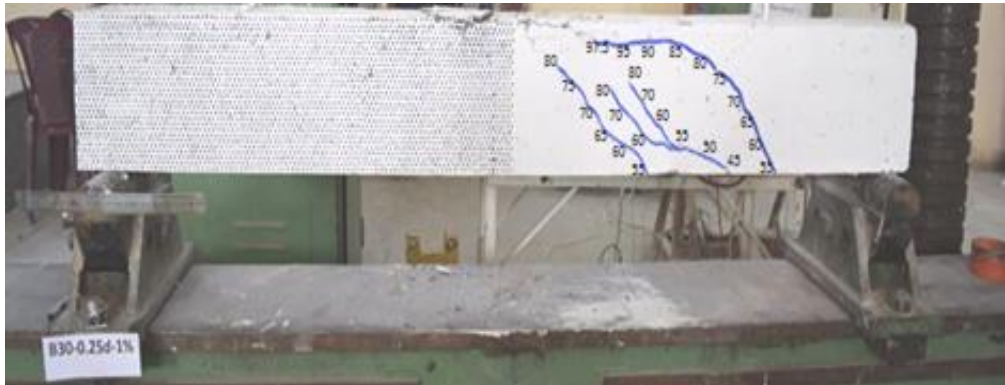


Figure 25: Crack pattern of beam (B30-0.25d-1)

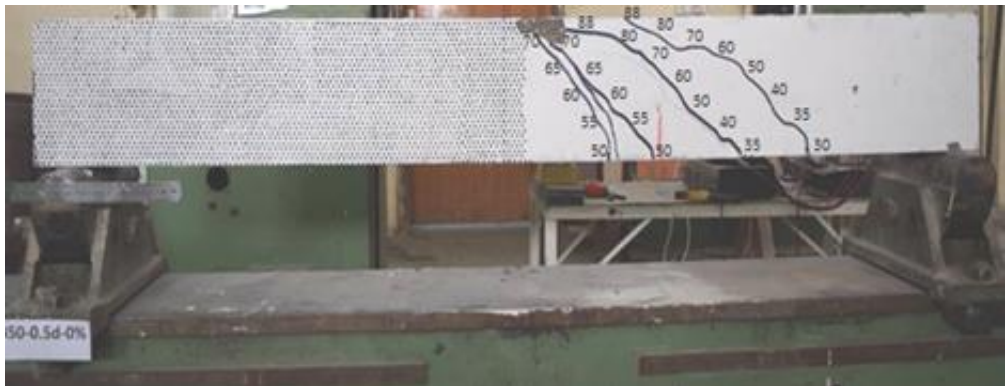


Figure 26: Crack pattern of beam (B50-0.5d-0)

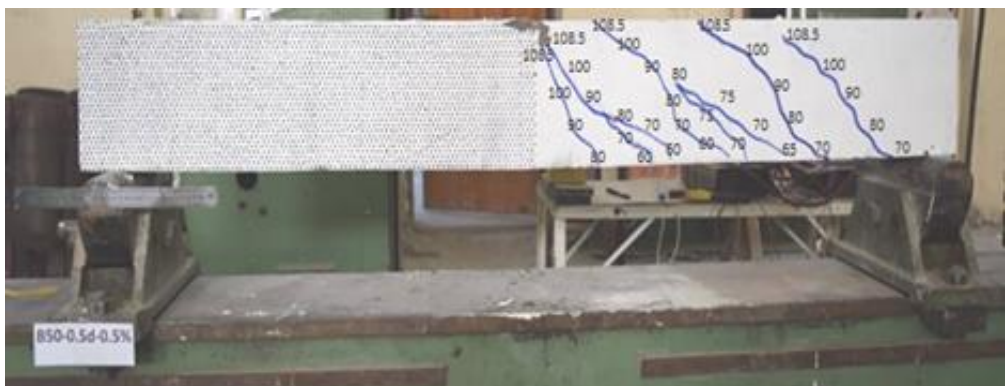


Figure 27: Crack pattern of beam (B50-0.5d-0.5)

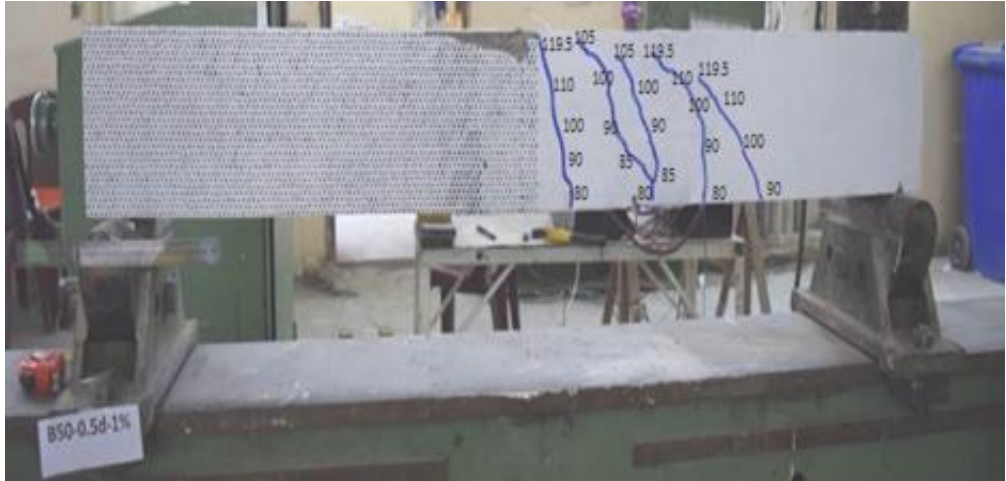


Figure 28: Crack pattern of beam (B50-0.5d-1)



Figure 29: Crack pattern of beam (B70-0.5d-0)

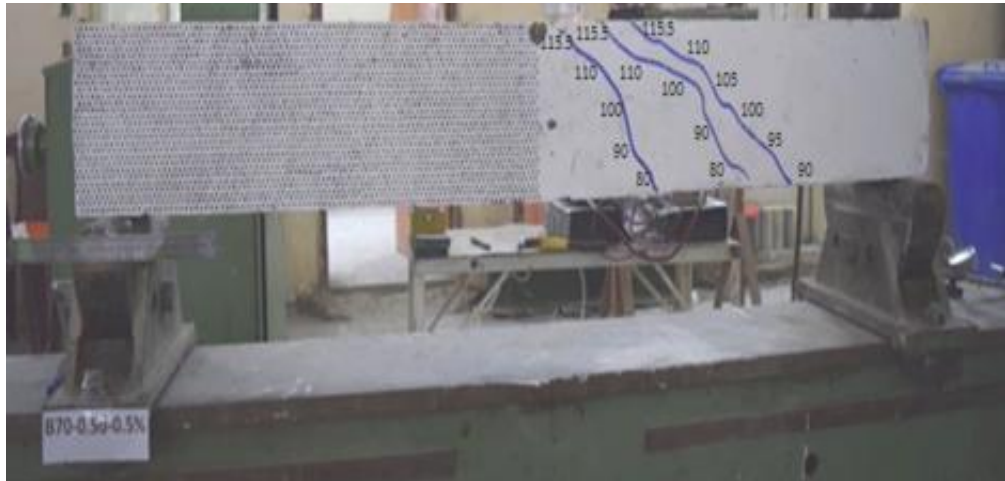


Figure 30: Crack pattern of beam (B70-0.5d-0.5)

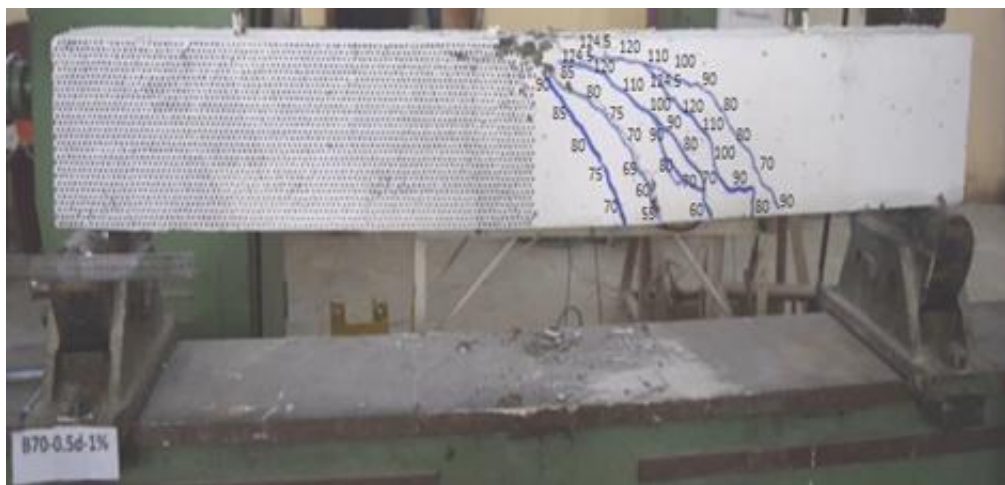


Figure 31: Crack pattern of beam (B70-0.5d-1)

9. Failure Mode

Table 6 summarized failure modes for all of the tested beams, results showed that increasing of steel fibers content from 0 to 1% change modes of the failure from shear to flexure-shear failure which is more safe and ductile, also increasing shear reinforcement ratio from 0.222 to 0.443% converts the modes of failure form shear to flexure-shear failure regardless of steel fibers content. However, the results showed that compressive strength of the concrete had no effect on failure modes; also the use of GFRP stirrups had no effect on failure modes as compared with reference beams.

Table 6: Experimental result and modes of failure

BS	ρ_{vf} (%)	f^c (MPa)	ICL	FL	Pcr/Pu	MSDF	MOF
BR30-0.5d-0 (Reference)	0.222	30	21.5	76.5	0.28	11.98	C.C+S.F
B30-0.5d-0			20	76	0.26	12.5	C.C+S.F
B30-0.5d-0.5	0.222	30	22	82.5	0.27	13.4	FF+S.F
B30-0.5d-1			23.5	87.5	0.268	11.8	FF+S.F
B30-0.33d-0			18.5	81	0.23	11.8	C.C+S.F
B30-0.33d-0.5	0.333	30	20	87.5	0.22	11.5	FF+S.F
B30-0.33d-1			22.5	92.5	0.24	11.9	FF+S.F
B30-0.25d-0			17.5	82	0.21	11.95	FF+S.F
B30-0.25d-0.5	0.443	30	21.5	90.5	0.23	12.85	FF+S.F
B30-0.25d-1			24	97.5	0.25	11.2	FF+S.F
B50-0.5d-0			24	88	0.27	10.8	S.F
B50-0.5d-0.5	0.222	50	25	108.5	0.23	9.98	FF+S.F
B50-0.5d-1			27	119.5	0.22	10.25	FF+S.F
B70-0.5d-0			24	97	0.25	11.1	S.F
B70-0.5d-0.5	0.222	70	26	115.5	0.23	11.4	S.F
B70-0.5d-1			27.5	124.5	0.22	10.6	F.F+S.F

*BS: Beam Specimen

ICL: Initial Crack Loading (Pcr) (kN)

FL: Failure Load (Pu) (kN)

MSDF: Midspan Deflection at Failure (mm)

MOF: Modes of Failure

C.C: Crushing of Concrete, S.F.: Shear Failure, FF: Flexural Failure

10. Theoretical Prediction of ultimate load

In the present study, the theoretical ultimate load V_u of GFRP reinforced beams was calculated according to the formulas supplied by shear design formulas to verify the validity of these formulas.

Table 7 lists experimental and calculated results of ultimate load. The calculation equations given by ACI440.1 R-15 [15] and CSA S 806-12 [16] and ISIS [14] and Tureyen [17] show a good agreement of the beams' flexural strength.

The CSA [16] and ISIS [14] codes showed conservative results while the ACI440-1R [15] and Tureyen [17] equation shows the good agreement in the result when compared with experimental results.

11. Conclusions

1. Increasing shear reinforcement ratio from 0.222% to 0.333% increases the failure load by 2, 6 and 5% for steel fiber content 0, 0.5 and 1%, respectively.
2. Increasing shear reinforcement ratio from 0.222% to 0.443% increases the failure load by 8, 10 and 11% for steel fiber content 0, 0.5 and 1%, respectively.
3. Increasing compressive strength of the concrete from 30MPa to 50MPa increases the failure load by 14, 32 and 37% for steel fiber content 0, 0.5 and 1% , respectively.
4. Increasing compressive strength of the concrete from 30MPa to 70MPa increases the failure load by 28, 40 and 42% for steel fiber content 0, 0.5 and 1% , respectively.
5. Increasing steel fiber content 0% to 0.50 and 1% increases the failure load by 8.5 and 15.1 % , respectively for beams with $\rho_{vf} = 0.222\%$.
6. Increasing steel fiber content 0% to 0.5 and 1% increases the failure load by 8 and 14.2 % , respectively for beams with $\rho_{vf} = 0.333\%$.
7. Increasing steel fiber content 0% to 0.5 and 1% increases the failure load by 10.4 and 18.9 % , respectively for beams with $\rho_{vf} = 0.443\%$.
8. The use of GFRP stirrups has very marginal effect on failure load
9. Results showed that the increase in the steel fibers contents from 0 to 1% change mode of failure from the shear into the flexure-shear failure which has been found more safe and ductile, also increasing the shear reinforcement ratio from 0.222 to 0.443% converts failure mode form shear to flexure-shear failure regardless of steel fibers content.
10. The increase in steel fibers content leads to decrease the strain in longitudinal GFRP bars between (4-56 %).
11. The increases in concrete compressive strength from 30 to 70 MPa decrease the strain in longitudinal GFRP bars between (40-74 %).
12. The increase in steel fibers content leads to decrease the strain in GFRP stirrups between (14-140 %).
13. The increases in compressive strength value of concrete from 30MPa to 70MPa decrease the strain in GFRP stirrups between (60-125%).

14. The increase in shear reinforcement ratio from 0.222 to 0.443 decreases the strain in stirrups GFRP bars between (5-64%).
15. Results showed that the increasing in steel fibers content reduce the deflection at an identical load level for all of the beams that have been tested.
16. Crack width were decreased by (35- 94%) when the steel fibers content increases from 0 to 1% for beam with $f'c = 30MPa$.
17. Crack width was decreased by (74-108%) when the steel fibers content increases from 0 to 1% for beam with $f'c = 50MPa$.
18. Crack width was decreased by (32-67%) when the steel fibers content increases from 0 to 1% for beam with $f'c = 70MPa$.
19. The calculated result showed that the CEB-FIP [67] have a good agreement with experimental result because the CEB-FIP [67] equation take in consideration the strain in longitudinal bars which effected by the parameters of study.
20. The comparison of experimental and calculated ultimate shear load showed that the CSA and ISIS codes result were very conservative with safety factor reach to 66%, whereas the ACI and Tureyen equation code results showed good agreement to the experimental results.

Table 7: Comparison of experimental and calculated ultimate loads

Beam Specimens	Vu (exp) (KN)	Vu (ACI) (KN)	Vu (CSA) (KN)	Vu (ISIS) (KN)
BR30-0.5d-0	38.25	38.67	24.3	28.58
B30-0.5d-0	38	38.67	24.3	28.58
B30-0.5d-0.5	41.25	40.05	25.29	29.63
B30-0.5d-1	43.75	41.07	26	30.42
B30-0.33d-0	40.5	49.08	26.54	36
B30-0.33d-0.5	43.75	50.45	27.53	37.05
B30-0.33d-1	46.25	51.47	28.3	37.84
B30-0.25d-0	40.25	59.5	28.79	43.43
B30-0.25d-0.5	45.25	60.85	29.78	44.48
B30-0.25d-1	48.75	61.87	30.52	45.27
B50-0.5d-0	44	43.49	27.71	32.28
B50-0.5d-0.5	54.25	45.2	28.86	33.58
B50-0.5d-1	59.75	46.57	29.76	34.64
B70-0.5d-0	48.5	47.73	30.52	35.53
B70-0.5d-0.5	57.75	48.84	31.22	36.38
B70-0.5d-1	62.25	49.82	32.84	37.13
Beam Specimens	$\frac{Vu_{exp}}{Vu_{ACI}}$	$\frac{Vu_{exp}}{Vu_{CSA}}$	$\frac{Vu_{exp}}{Vu_{ISIS}}$	$\frac{Vu_{exp}}{Vu_{Tureyen}}$
BR30-0.5d-0	0.99	1.57	1.34	1.10
B30-0.5d-0	0.98	1.56	1.33	1.1
B30-0.5d-0.5	1.03	1.63	1.4	1.11
B30-0.5d-1	1.07	1.68	1.43	1.11
B30-0.33d-0	0.83	1.53	1.13	1.17
B30-0.33d-0.5	0.87	1.59	1.18	1.17
B30-0.33d-1	0.9	1.63	1.22	1.18
B30-0.25d-0	0.67	1.4	0.93	1.16
B30-0.25d-0.5	0.74	1.52	1.02	1.21
B30-0.25d-1	0.79	1.59	1.08	1.24
B50-0.5d-0	1.01	1.59	1.36	1
B50-0.5d-0.5	1.2	1.88	1.62	1.15
B50-0.5d-1	1.3	2	1.72	1.2
B70-0.5d-0	1.02	1.59	1.37	0.93
B70-0.5d-0.5	1.18	1.85	1.59	1.06
B70-0.5d-1	1.25	1.89	1.68	1.11
average	0.99	1.66	1.34	1.12

12. References

- [1] Emile F.G. Shehata, (1990) "FIBER-REINFORCED POLYMER (FRP) FOR SHEAR REINFORCEMENT IN CONCRETE STRUCTURES", ph.D Thesis, University of Manitoba, Canada.
- [2] Bell, T. (n.d.). (2018) ,How and Why Do Metals Corrode? Retrieved May 31, from <https://www.thebalance.com/what-is-corrosion-2339700>.
- [3] ACI Committee 222, "Protection of Metals in Concrete against Corrosion (ACI 222R-01)," ACI Manual of Concrete Practice, American Concrete Institute, Farmington Hills, MI.
- [4] The international Handbook of FRP COMPOSITES IN CIVIL ENGINEERING. Edited by Manoochehr Zoghi.
- [5] P. Balagury, A. Nanni, and J. Giancaspro, (2009), FRP Composites For Reinforced And Prestressed Concrete Structures, 1st ed. Taylor & Francis.
- [6] Japan Society of Civil Engineers (1997). Recommendation for design and construction of concrete structures using continuous fiber reinforcing materials. Concrete Engineering Series 23; Tokyo, Japan Society of Civil Engineers.
- [7] ASCE-ACI Committee 426, (1973); "Shear Strength of Reinforced Concrete Members", ASCE Proceedings, Vol. 99. 3T6, June, pp. 1091-1188.
- [8] ACI Committee 318, (2019) ; "Building Code Requirements for Reinforced Concrete and Commentary. American Concrete Institute. Detroit.
- [9] ASCE-ACI Committee 445 on Shear and Torsion, (1998); "Recent Approaches to Shear Design of Structural Concrete," Journal of Structural Engineering. ASCE, Vol.i24. No. 12. December. pp. 1375-1417.
- [10] Loov, R., (1998); "Review of A23.3-94 Simplified Method of Shear Design and Comparison with Results Using Shear Friction, " Canadian Journal of Civil Engineering, Vol. 25. No. 3,june, pp.437-150.
- [11] Hassan, Hassan F., and Muayad M. Abdullah. "FLEXURAL BEHAVIOR OF NORMAL AND HIGH STRENGTH CONTINUOUS BEAMS REINFORCED BY GFRP BARS."
- [12] American Concrete Institute. Committee 440. (2006), "Guide for the Design and Construction of Concrete Reinforced with FRP Bars: ACI 440.1 R-06." American Concrete Institute.

- [13] CEB-FIP. ; (2007) FRP reinforcement in RC structures. Fib bulletin 40. International Federation for Structural Concrete (fib).
- [14] ISIS Canada, (2007) Reinforcing Concrete Structures with Fiber Reinforced Polymers. Design Manual N8 3 Version 2, Canada ISIS Canada Corporation, Manitoba.
- [15] ACI (American Concrete Institute). (2015). "Guide for the design and construction of structural concrete reinforced with FRP bars." ACI 440.1R-15, Farmington Hills, MI.
- [16] CSA, S806-12: (2012), Design and Construction of Building Components with Fiber-Reinforced Polymers, Canadian Standards Association, Canada.
- [17] El-Sayed AK, El-Salakawy EF, Benmokrane B (2006b) Shear strength of normal strength concrete beams reinforced with deformed GFRP bars. ACI Struct J 103(2):235–24a.

سلوك القص للعتبات الخرسانية الليفية المسلحة بالألياف الزجاجية البوليمرية

علي السجاد ابراهيم جواد¹
ali199963110@gmail.com

حسن فلاح حسن²
hassanfalah@uomustansiriyah.edu.iq

محمد حسين كلظم³
mohammed.aldahlalei@gmail.com

المستخلص: يمكن استخدام "البوليمرات المقواة بالألياف الزجاجية" (GFRP) لإنتاج قضبان التسليح التي يمكن استخدامها كبديل جيدة للفولاذ التقليدي نظراً لنسبة القوة / الوزن المعقولة ومقاومة التآكل. "الخرسانة المسلحة بالألياف" (FRC) هي نوع من الخرسانة التي يمكن تصنيعها بإضافة ألياف فولاذية إلى مزيج الخرسانة من أجل تعزيز الخواص الميكانيكية والأداء الهيكلي الناتج. قدمت هذه الدراسة لفحص أداء القص للعتبات الخرسانية الليفية المسلحة بقضبان GFRP للنتاء والقص. تضمنت هذا الدراسة صب ستة عشر عتبة من الخرسانة المسلحة. تم تسليح خمس عشرة عتبة بواسطة قضبان GFRP وتم تسليح عتبة واحدة بواسطة قضبان فولاذية كعتبة مرجعية. تضمنت هذه الدراسة عدة متغيرات وهي نسبة الألياف الفولاذية ونسبة قضبان القص ومقاومة الانضغاط للخرسانة، وتم تقسيم النماذج إلى خمس مجموعات وفقاً لمعايير الاختبار. أظهرت النتائج التجريبية أن زيادة نسبة قضبان القص من 0.444 % إلى 0.887 % يزيد من حمل الفشل بنسبة 8 و 9 و 11 % لمحتوى ألياف الفولاذ 0 و 0.5 و 1 % على التوالي. كما أظهرت النتائج أن زيادة مقاومة الانضغاط للخرسانة (30-70 MPa) يزيد من حمل الفشل بنسبة 27 و 40 و 42 % لمحتوى ألياف الفولاذ 0 و 0.5 و 1 % على التوالي. تؤدي زيادة مقاومة الانضغاط للخرسانة (30-70 MPa) إلى تقليل الضغط زيادة حمل الفشل بنسبة 8 إلى 18.9 %. تؤدي زيادة مقاومة الانضغاط للخرسانة (30-70 MPa) إلى تقليل الضغط في قضبان GFRP الطولية بنسبة تتراوح بين (60-125) %، بينما تؤدي زيادة نسبة قضبان القص من 0.444 إلى 0.887 إلى تقليل الإجهاد في قضبان GFRP الطولية بين (5-64) %. أدت الزيادة في نسبة الألياف الفولاذية إلى انخفاض في إجهاد الخرسانة الانضغاطي بين (5.71-30.1) %. زيادة مقاومة الانضغاط للخرسانة (30-70 MPa) ينقص في إجهاد الانضغاط الخرساني بنسبة (8.25 - 26.9) %. انخفاض عرض التشققات بنسبة (32-108) % عند زيادة نسبة ألياف الفولاذ من 0 إلى 1 % لجميع العينات. أظهرت النتائج التجريبية أن زيادة محتوى ألياف الفولاذ ونسبة تسليح القص تقلل من إجهاد الانضغاط النهائي للخرسانة. أظهرت النتائج أن مؤشر المطيلية بطريقة التشوه يتناقص مع زيادة محتوى الألياف الفولاذية نتيجة زيادة العزم والانحراف عند $(\epsilon_{cu}=0.001)$. أظهرت مقارنة حمل القص النهائي التجريبي والمحسوب أن نتيجة معادلة CSA و ISIS كانت متحفظة للغاية حيث وصل عامل الأمان إلى 66 %، بينما أظهرت نتائج كود معادلة ACI و Tureyen توافقاً جيداً مع النتائج التجريبية.

الكلمات المفتاحية: الخرسانة المسلحة بالألياف، البوليمرات المقواة بالألياف الزجاجية، عتبات خرسانية، تسليح

¹ طالب ماجستير: قسم الهندسة المدنية - كلية الهندسة - الجامعة المستنصرية - بغداد - العراق

² أستاذ دكتور: قسم الهندسة المدنية - كلية الهندسة - الجامعة المستنصرية - بغداد - العراق

³ أستاذ مساعد دكتور: قسم الهندسة المدنية - كلية الهندسة - الجامعة المستنصرية - بغداد - العراق